Second harmonic generation by artificial chiral materials

Mario Bertolotti,[1] Alessandro Belardini [1], Alessio Benedetti ,[1] Concita Sibilia [1*]

[1] *Università di Roma La Sapienza, Dipartimento SBAI, Via Scarpa 16, 00161 Roma, Italy*

**Corresponding author: concita.sibilia@uniroma1.it*

It is possible to realize artificial chiral structures in the optical domain thanks to the recent successes in nanotechnology. A 2D and/or 3D chiral configuration can be artificially realized, opening the way to new functionalities on a spatial scale of few hundred on nms. The second order nonlinear response of nanostructured materials is an interesting and fascinating issue. In artificial chiral materials it takes advantage of the mutual interaction among electric and magnetic nonlinear response. In the present paper we report an overview of second harmonic generation raised by artificial chiral structures of different morphologies and material components.

OCIS codes: (190.4400) Nonlinear Optics, materials; (240.4350) Nonlinear Optics at the surfaces;(240.6680) Surface plasmons.

1.Introduction

Chirality has become a very much studied property due to its potential applications in different areas, as analytical chemistry, crystallography, molecular biology, and new chiral materials may find application for example in polarization control devices. Systems that cannot be superposed to their mirror image are said to be chiral, the word chirality deriving from the Greek, χειρ, which means hand, that is the most familiar chiral object. A chiral object and its mirror image are called enantiomorphs (Greek, opposite forms εναντιος plus μορφη) or, when referring to molecules, enantiomers. The term was first used by Lord Kelvin [1] and chirality is a property of asymmetry.

From the optical point of view, chiral structures possess the ability to rotate the plane of polarization of electromagnetic waves (optical activity), and give rise to dichroism (again from the Greek δικρως, two-colored) that is the property to split a beam of light into two beams with different wavelengths. A dichroic material is either one which causes visible light to be split up into distinct beams of different wavelengths (dichroic mirrors) or one in which light rays having different polarizations are absorbed by different amounts. When the polarization states in question are right and left-handed circular polarization, one refers to circular dichroism.

It has been predicted and demonstrated [2,3,4] that strong enough optical activity may result in negative refraction and reflection, and this has further fostered research in new chiral schemes.

Some complex molecules are chiral, as for example sucrose, and most chiral molecules are bio-molecules.

Optical activity effects arise from different interactions of chiral molecules with left and right-hand circular polarized light. Conventional optical activity effects, such as circular dichroism and polarization rotation, arise from molecular chirality and occur in isotropic bulk liquids (e.g. sugar solutions) and molecular crystals.

Circular dichroism may be obtained also by using metamaterials. For example it is possible to obtain a chiral behavior by engineering the elementary cell of a periodic structure with a chiral arrangement of non-chiral objects (intrinsic chirality or structural chirality).

Recent nanofabrication techniques have made it possible to prepare samples with so-called planar or two-dimensional chirality. Very strong optical activity has been demonstrated in a metamaterial [5] system consisting of molecules that by itself are not chiral but chirality is drawn extrinsically from the mutual orientation of the wave propagation direction and the two dimensional metamaterial. The effect can be seen when oriented non-chiral molecules make a chiral triad with the wavevector of light (extrinsic chirality). This mechanism was first described by Bunn [6] and detected in liquid crystals [7].
The arising of chiral behavior due to proper alignment of achiral samples with respect the measurement setup was originally discovered and studied in the linear optics regime and is present also in non-linear optics, in particular in the case of second harmonic generation. Strong chirality in metamaterials has been studied by several authors [8,9,10,11].
In the following, we will discuss some cases of second harmonic generation by artificial chiral materials, considering different structures: straight metallic wires, curved metallic wires and partially metallized spheres, showing the importance of the geometry of the experimental disposition.

2. General considerations about chirality

Chiral molecules have no reflection or inversion symmetry and occur in two forms (enantiometers) that are mirror images one of each other. They interact differently with left- and right-hand circularly polarized light [12] . As light traverses the medium, the differences in the real parts of the refractive indices lead to the rotation of the plane of polarization, while the differences in the imaginary parts lead to circular dichroism. In isotropic solutions of chiral molecules, optical activity effects arise from magnetic contributions to the linear optical response and are usually relatively weak. Second-order processes have been revised recently [13] and may be explained including magnetic contributions to the second order response [14] .

To describe the chiral response it is convenient to write the constitutive relations between $\vec{\boldsymbol{E}}$, $\vec{\boldsymbol{D}}$, $\vec{\boldsymbol{B}}$ and $\vec{\boldsymbol{H}}$ using the temporal Fourier transforms, so that the frequency-domain constitutive relations can be expressed as

$$\begin{aligned}\vec{D}(\omega) &= \varepsilon\vec{E}(\omega) - jk\sqrt{\varepsilon_0\mu_0}\,\vec{H}(\omega)\\ \vec{B}(\omega) &= jk\sqrt{\varepsilon_0\mu_0}\,\vec{E}(\omega) + \mu\vec{H}(\omega)\end{aligned} \tag{1}$$

For a homogeneous, isotropic chiral medium the space dependence of ε and χ is obviously missing [15,16].
Writing down the appropriate solutions of Maxwell equations [17], plane waves in an isotropic chiral medium must be circularly polarized.
Assuming propagation along the z axis one finds two solutions in the form of a right circular polarization state and a left polarization state

$$\begin{aligned}\vec{E} &= A(\hat{u}_x - j\hat{u}_y)exp[-jk_0(N-k)z]\\ \vec{H} &= j\left(\sqrt{\varepsilon/\mu}\,A(\hat{u}_x - j\hat{u}_y)\right)exp[-jk_0(N-k)z]\end{aligned} \tag{2}$$

that is a right circular polarized wave and

$$\begin{aligned}\vec{E} &= C(\hat{u}_x + j\hat{u}_y)exp[-jk_0(N+k)z]\\ \vec{H} &= j\left(\sqrt{\varepsilon/\mu}\,C(\hat{u}_x + j\hat{u}_y)\right)exp[-jk_0(N+k)z]\end{aligned} \tag{3}$$

that is a left circular polarized wave, being $N = \sqrt{\varepsilon_r\mu_r}$, A and C two suitable constants , $j = \sqrt{-1}$, k the chiral parameter, $k_0=\omega/c$, and $\hat{u}_x$, $\hat{u}_y$ the unitary vectors in the x and y directions.
These fields propagate with wavevectors

$$\begin{aligned}k_1 &= \omega\left\{\sqrt{\varepsilon(\omega)\mu(\omega)} - k\right\}\\ k_2 &= \omega\left\{\sqrt{\varepsilon(\omega)\mu(\omega)} + k\right\}\end{aligned} \tag{4}$$

Since $k_1 \neq k_2$, the left and right circularly polarized plane wave propagate with different phase velocities and with different attenuation rates, so the material is circularly birefringent.
From a simple morphological point of view we may consider a 3D chiral object in front of a mirror parallel to the plane x,y and describe the mirror action on a point object P(x,y,z) through a mirror matrix M which has elements

$$M = \begin{pmatrix} -1 & 0 & 0 \\ 0 & 1 & 0 \\ 0 & 0 & -1 \end{pmatrix} \tag{5}$$

The final coordinates of a point P(x,y,z) are therefore

$$\begin{pmatrix} -x \\ y \\ -z \end{pmatrix} = M \begin{pmatrix} x \\ y \\ z \end{pmatrix} \tag{6}$$

We may therefore say that the object is non-chiral if it possess an inversion symmetry around the y-axis.
To be chiral, a body must not contain any rotation-reflection axis. In other words, it may have neither symmetry planes, nor any center of inversion, nor any higher rotation-reflection symmetry.
For example, a helix in the example of fig.1 is a chiral object; in the figure 1, the z axis is vertical.

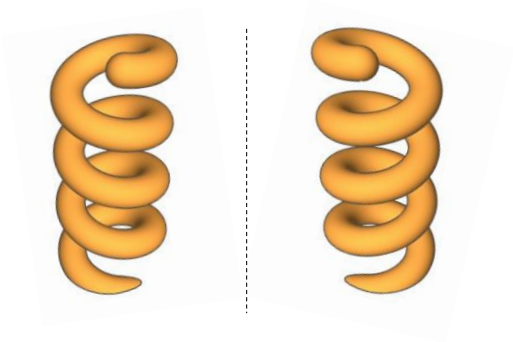

Figure 1: Example of chiral structure: the helix.

Typically, biological molecules present a chiral morphology, and by the optical point of view, they exhibit the property of rotating the polarization plane of an incident linearly polarized light.

3 Dichroism in artificial nanostructures

In the following we present few examples of extrinsic chirality considering straight and tilted gold nanowires self-assembled on dielectric or semiconductor substrates, and self-ordered dielectric nanospheres partially covered by gold nano crescents. We note that extrinsic chirality arose when the sample is considered from the extrinsic point of view of the incoming light.

Let us first consider self assembled gold nanowires. We may first consider a sample made of parallel nanowires lying on a plane substrate (fig.2).

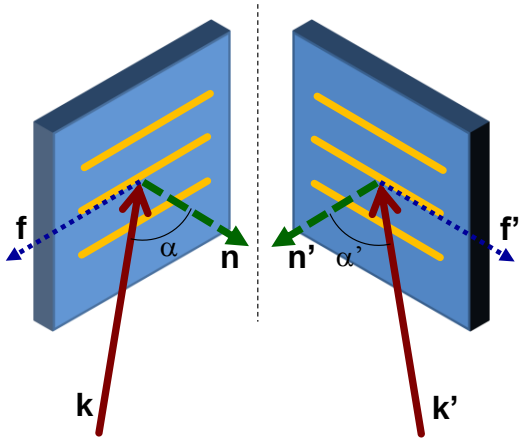

Figure 2: Non chiral disposition of wires; a triad formed by the normal to the surface **n** (green arrow), the vector **f** in the direction of the wires (blue arrow) and the incoming wave with wavevector **k** (red arrow) is considered. A rotation of 180° around **k'** restores the original triad showing that the structure is not chiral .

We consider a triad of three vectors: the normal to the surface **n** (green arrow), a unit vector **f** in the direction of the wires (blue arrow in fig.2) and an incoming wave with wavevector **k** (red arrow), We assume that the direction **f** of the wires lies in the incidence plane (**k,n**) and also lies on the substrate surface ($\boldsymbol{f} \cdot \boldsymbol{n} = 0$). The **k** vector is forming an angle α with respect to the normal **n.** We may apply the considerations developed previously to find that the mirror image looks as shown in fig.2. In particular the reflected triad **n' f' k'** has the **f'** vector (blue arrow) pointing in the opposite direction and the α' angle lies on the other side of the normal **n'**. However a rotation of 180° around the direction of light **k=k'** restores the original triad symmetry showing that the structure is not chiral. We remind the reader that when we are speaking about extrinsic chirality we refer to the symmetries of the sample considered from the incoming light point of view that is an extrinsic point of view and not to the intrinsic symmetries of the sample by itself, that's way we can state **k=k'**. The same considerations can be applied to the case in which the nanowires form an angle with the substrate plane but remaining in the (**k,n**) plane, as shown in fig.3.

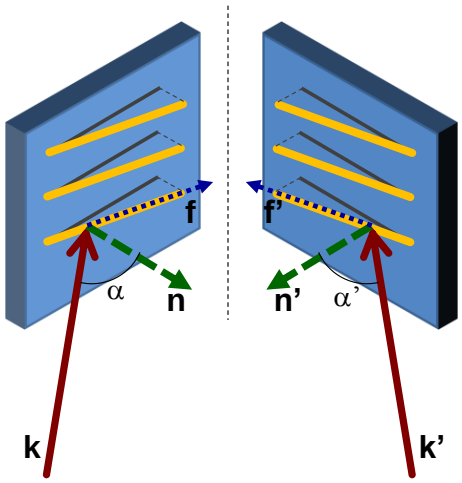

Figure 3: Non chiral disposition of wires; consider the triad formed by the normal to the surface **n** (green arrow), the vector **f** in the direction of the wires (blue arrow) and the incoming wave with wavevector **k** (red arrow). Even if the wires are tilted with respect to the substrate, their direction still lie in the (**k,n**) plane, this implies that a rotation of 180° around **k'** restores the original triad showing that the structure is not chiral .

However if the direction of the wires **f** lies out of the incidence (**k, n**) plane (fig.4), after reflection the triad is changed.

No rotation around the light direction or translation is able, in this case, to reproduce the original triad and the setup results to be chiral.

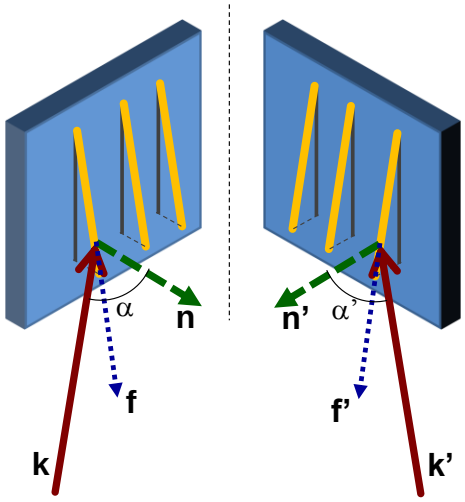

Figure 4: chiral disposition of wires; the triad is formed by the normal to the surface **n** (green arrow), the vector **f** in the direction of the wires (blue arrow), that are tilted with respect the surface of the sample and the incoming wave with wavevector **k** (red arrow). A rotation of 180° around **k'** doesn't restore the original triad showing that the structure behaves as chiral.

Now we consider curved nanowires lying in the plane of the substrate, we may use the radius of curvature of the semicircular nanowires as the **f** vector defining the structure. With reference to the fig.5 we see that in the case when the radius of curvature is outside the plane of incidence (**k,n**) the sample behaves as a chiral sample.

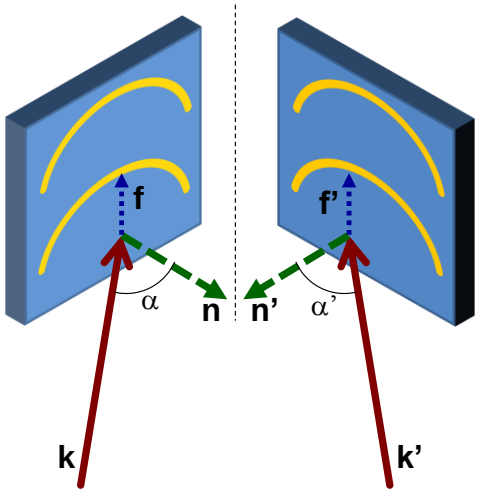

Figure 5: Chiral disposition of wires : the triad is formed by the normal to the surface **n** (green arrow), the vector **f** representative the direction of the wires radius of curvature (blue arrow) and the incoming wave with wavevector **k** (red arrow). A rotation of 180° around **k'** does not restore the original tern showing that the structure is chiral.

In figure 6 we show a different disposition of the same sample. In this case the radius of curvature, represented by the unit vector **f,** is in the plane of incidence (**k,n**) and the sample behaves as a non-chiral sample (from the extrinsic point of view of the incoming light).

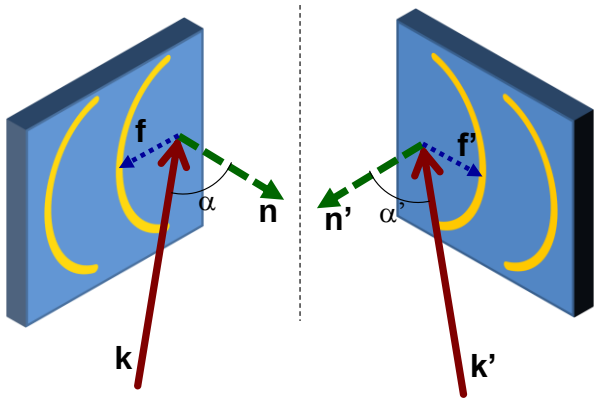

Figure 6: Non chiral disposition of the curved wires; the triad is formed by the normal to the surface **n** (green arrow), vector **f** representative the direction of the wires radius of curvature (blue arrow) and incoming wave with wavevector **k** (red arrow). A rotation of 180° around **k'** restores the original tern showing that the structure is not chiral.

More complex structures are depicted in figure 7 where asymmetric gold nano-crescent were growth on a system of polystyrene spheres on a dielectric substrate. Still in this case the artificial chirality rises from the direction of the impinging light wavevector **k** (red arrow) with respect to the normal unit vector **n** (green arrow) and the direction **f** representative of the asymmetric gold geometry. In this case, both the geometrical setup (extrinsic chirality) and the elementary cell are chiral (intrinsic chirality). The gold crescent can be obtained in real cases[18-19] by evaporating gold, from a specific direction represented by the vector **f,** on a substrate formed by polystyrene spheres.

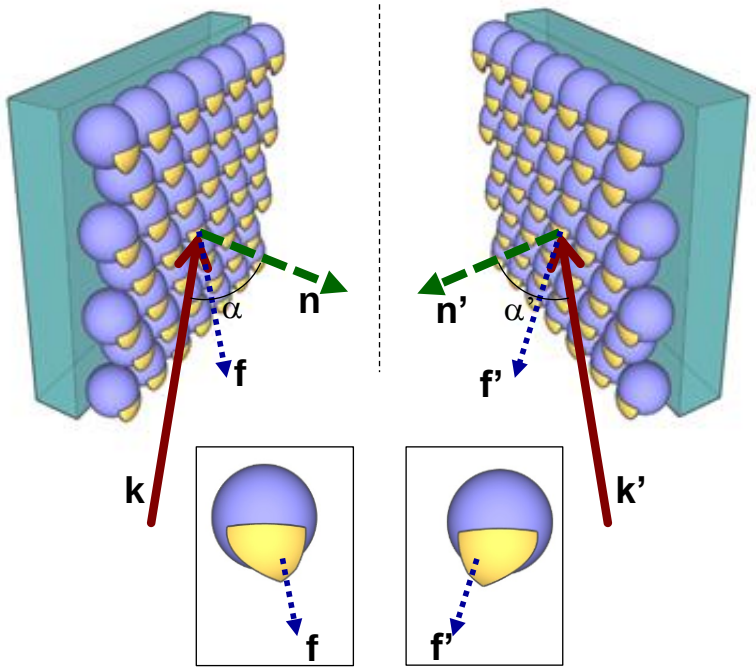

Figure 7 – Nanosphere with gold crescents as artificial chiral structure.

In is possible to obtain similar structures but with different gold symmetries depending on gold vapor flux direction with respect to the spheres geometry[20] (see. Fig.8).

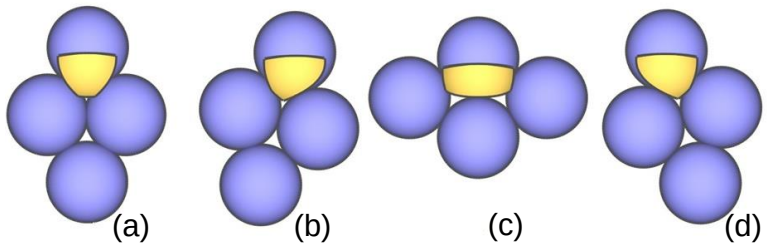

Figure 8 – Different gold geometries due to the reciprocal gold vapor flux – spheres orientation during sample fabrication. Structures (a) and (c) are symmetric structure meanwhile (b) and (d) are one the enantiomer of the other.

In fig.8 are shown gold symmetric structure (fig.8a and fig.8c) and also asymmetric structures (fig.8b and fig.8d). The asymmetric structure are chiral from the extrinsic point of view and result to be one the enantiomer form of the other[20].

4. Experimental results

A very sensitive method to experimentally investigate symmetry properties of metasurfaces is the optical second harmonic generation (SHG), in particular the chiral behavior of nanostructures can be addressed as described in ref. 21. Chirality in second order nonlinear optical processes ads a number of independent components of the susceptibility tensor. For the case of chiral isotropic in the plane of the substrate (symmetry group C∞), reflection symmetry with respect to planes containing the surface normal is broken. This introduces additional components (xyz = xzy = -yzx = -yxz) already in the electric-dipole-allowed susceptibility tensor $\chi^{(2)}$. In-plane anisotropy complicates the situation even further as the coordinates x and y must be chosen in a system tied to the sample.
One useful parameter describing the chirality of a sample is the second harmonic generation circular dichroism[21] (SHG-CD) defined as the difference between the generated SH field intensity (at *s* or *p* polarization state) obtained from the left-handed circular polarized light and the right-handed one divided by the average total generated intensity:

$$SHG\text{-}CD = \frac{I_L^{2\omega} - I_R^{2\omega}}{(I_L^{2\omega} + I_R^{2\omega})/2} \tag{7}$$

An experimental disposition to study chirality in second harmonic generation is the one describe in fig.9 in which the fundamental light at the wavelength of 800nm is impinging at a incidence angle α on the sample under study. The input light polarization is set either on left-handed polarization state (L) or right-handed one (R) by a quarter wavelength retarder plate. The second harmonic generated signal is analyzed in the *p* polarization state (p) by a polarizer. By rotating the polarizer, it is also possible to measure the *s* polarization state (s).

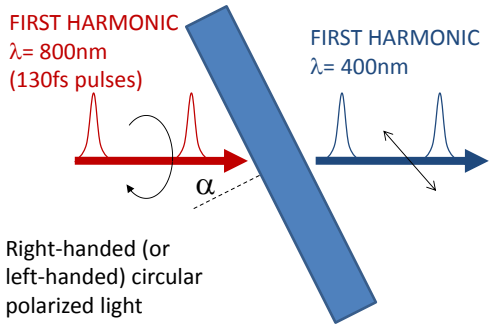

Figure 9: experimental setup able to detect the second harmonic circular dichroism (SHG-CD) of a sample.

I fig.10 we show the measurements of SHG-CD obtained on a sample of straight gold nanowires on a glass substrate[22]. As expected by symmetry reasons described in fig,2 the SHG-CD results to be zero and no chirality is present.

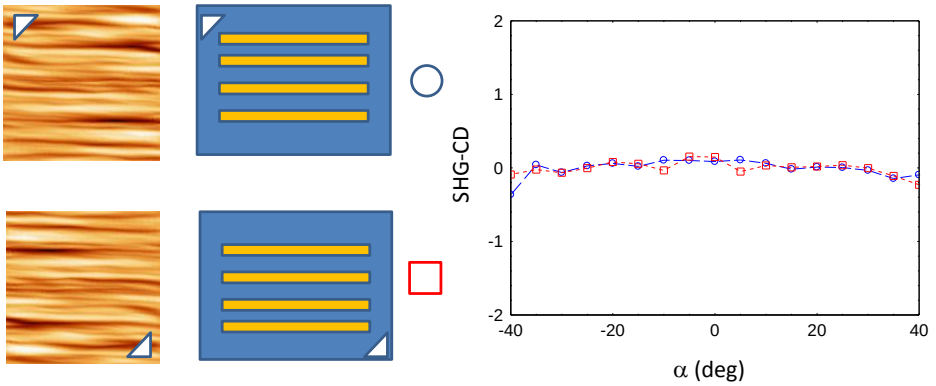

Figure 10: on the left the atomic force microscopy (AFM) image of the sample with the relative schematic of the wires orientation and the corresponding mark in the measurements (blue circle for the sample oriented in one direction, red square when the sample is rotated by 180° around its normal) ; on the right-side the SHG-CD measurements in p pol. state as a function of the incidence angle[22]. With this symmetry no chirality is present.

In fig.11, we show the measurements of the SHG-CD on a sample of curved gold nanowires on a glass substrate[22]. The disposition of the wires are similar to the ones in fig.6 so, also in this case, no chirality is present.

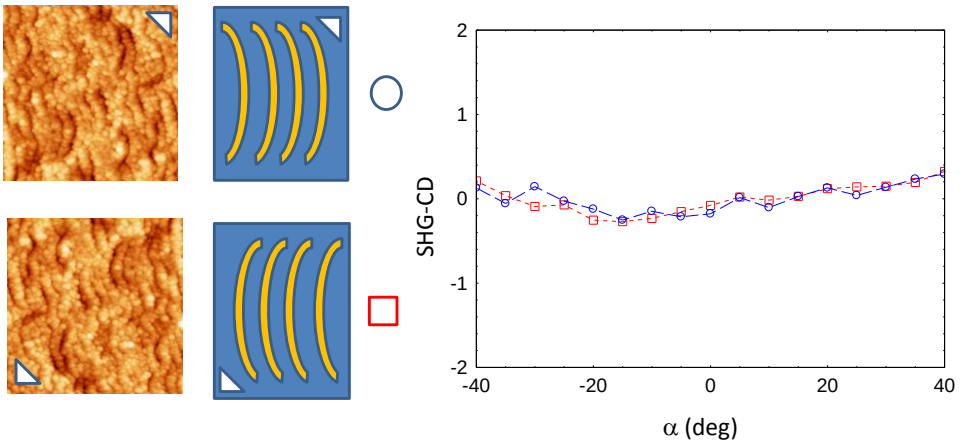

Figure 11: on the left the AFM image of the sample with the relative schematic of the wires orientation and the corresponding mark in the measurements (blue circle for the sample oriented with the radius of curvature of the wires pointing the right direction, red square when the sample is rotated by 180° around its normal, so with the radius of curvature pointing left) ; on the right-side the SHG-CD measurements in p pol. state as a function of the incidence angle[22]. Also with this symmetry no chirality is present.

In fig.12 we show the measurements[22] on the same sample of fig.11 , but with a different symmetry. The sample is rotated by 90° around its normal in order to have the radius of curvature of the wires laying outside the incidence plane. In this case the symmetry is similar to the one reported in fig.5 and the chirality is present.

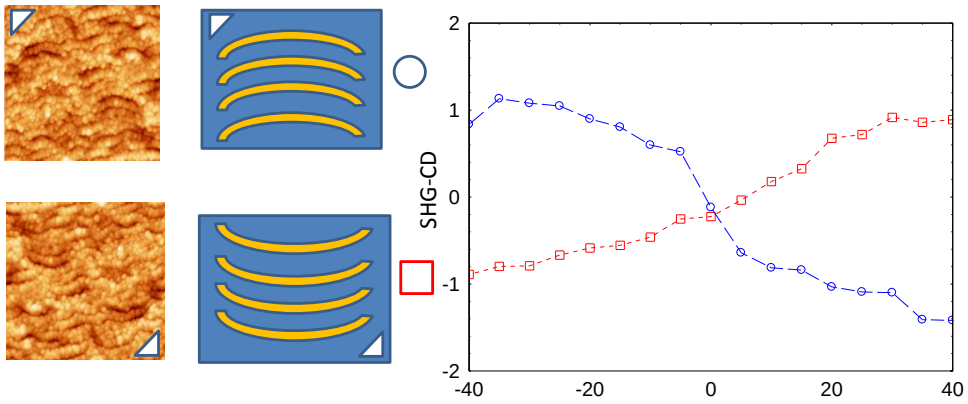

Figure 12: on the left the AFM image of the sample with the relative schematic of the wires orientation and the corresponding mark in the measurements (blue circle for the sample oriented with the radius of curvature pointing up, red square when the sample is rotated by 180° around its normal, so with the radius of curvature pointing down) ; on the right-side the SHG-CD measurements in p pol. state as a function of the incidence angle[22]. In this case the symmetry gives chiral response.

It is interesting to observe that at normal incidence (α=0) the chiral response of the sample in fig.12 is zero because the three vectors **k,n,f** of fig.5 in that particular case became coplanar. The absence of chiral response at zero degree indicates that the observed chirality is merely an extrinsic chirality raised by the relative orientation of sample and light direction. By scanning the incidence angle from negative to positive values, the triad **k,n,f** change its handedness and consequently the SHG-CD signal chance the sign. A similar effect is obtained by rotating the sample by 180° around its normal, in fact also in this case the **k,n,f** triad change the handedness because the **f** vector passes from one side of the incidence plane to the other.

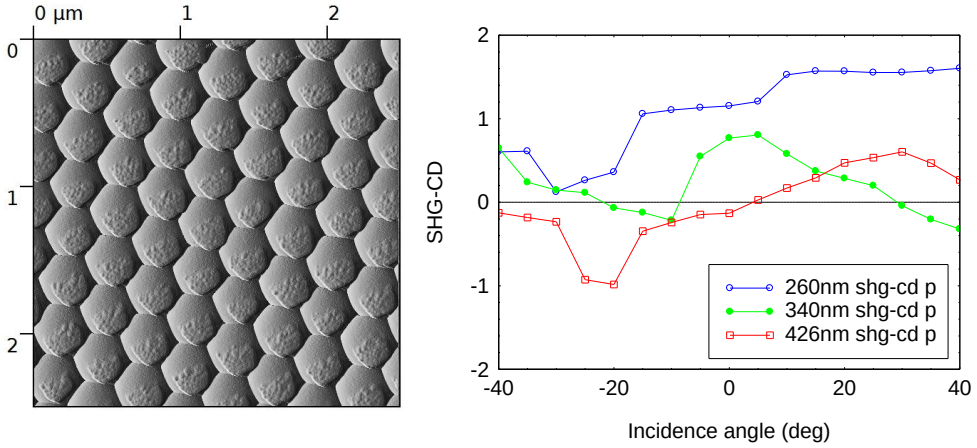

Figure 13: on the left scanning electron microscopy (SEM) image of a sample of polystyrene nanospheres with gold nanoantennas on the top; on the right-side the SHG-CD measurements[18] in p pol. state of samples with 260, 340, 426 nm diameter spheres (blue circles, green disks, red squares respectively).

In fig.13 we show the measurements[18] of the SHG-CD on samples formed by gold nanoantennas growth on polystyrene nanospheres deposited on a glass substrate as shown schematically in fig.7. Three samples were measured with three different spheres diameters, 260, 340, 426 nm. Due to the intrinsic asymmetry of the gold, as shown in fig.8, the chirality is present even at normal incidence. This fact indicates that in these samples there are a competition in the optical response between extrinsic chirality and intrinsic chirality.
In ref.23 we measures the SHG-CD of tilted gold nanowires as the ones described in fig.3 and fig.4. In this case chirality is observed[23] when the wires are mainly oriented in the vertical direction as described in fig.4, meanwhile when the sample is rotated by 90° around its normal, like the scheme in fig.3 the chirality is not present as expected.

5. Conclusions

The second harmonic generation process, like other second order effects, is critical dependent on the symmetry of the involved parameters. It results to be very sensitive to the symmetry breaking at the interfaces of investigated samples and particularly it results to be order of magnitude much sensitive about the chiral behavior of nanostructures with respect analogue linear optical measurements[22]. In this work, we show applications of second harmonic generation in the investigation of different self-assembled nanostructured samples. The intrinsic as well the extrinsic symmetries of the structures under study can be easily addressed sowing the potential of such technique in the field of nanotechnology characterization.

Acknowledgements

This work was partially financed by MARINE project granted by Italian Ministry of Defence.

References

1. Kelvin, W. Thomson, *The Molecular Tactics of a Crystal*, Clarendon Press, Oxford (1894).
2. A. V. Rogacheva, V. A. Fedotov, A. S. Schwanecke, and N. I. Zheludev, Phys. Rev. Lett. 97, 177401 (2006).
3. E. Plum, J. Zhou, J. Dong, V. A. Fedotov, T. Koschny, C. M. Soukoulis, and N. I. Zheludev, Phys. Rev. B 79, 035407 (2009).
4. S. Zhang, Y.-S. Park, J. Li, X. Lu, W. Zhang, and X. Zhang, Phys. Rev. Lett. 102, 023901 (2009).
5. E. Plum, X.-X. Liu, V. A. Fedotov, Y. Chen, D. P. Tsai, and N. I. Zheludev, Phys. Rev, Lett. 102, 113902 (2009).
6. C. W. Bunn, *Chemical Crystallography*, Oxford Univ. Press, New York, (1945).
7. R. Williams, Phys. Rev. Lett. 21, 342 (1968).
8. J. B. Pendry, Science 306, 1353 (2004).
9. M. Decker, M. W. Klein, M. Wegener, S. Linden, Opt. Lett. 32, 856 (2007).
10. J. K. Gansel, M. Thiel, M. S. Rill, M. Decker, K. Bade, V. Saile, G. von Freymann, S. Linden, and M. Wegener, Science 325, 1513 (2009).
11. M. Wegener and S. Linden, Physics 2, 3 (2009).
12. L. D. Barron, *Molecular Light Scattering and Optical Activity*, Cambridge Univ. Press, Cambridge (2004).
13. S. Cattaneo, M. Siltanen, F. Xiang Wang, M. Kauranen, Opt. Express 13, 9714 (2005).
14. M. Kauranen, S. Cattaneo, Progress in Optics 51, 69-120 (2008).
15. A. Lakhtakia, *Beltrami Fields in Chiral Media*, World Scientific, Singapore (1994).
16. T. G. Mackay and A. Lakhtakia, Progress in Optics 51, 121 (2008).
17. J. G. Van Bladel, *Electromagnetic Fields*, Wiley (2007).
18. A. Belardini, A. Benedetti, M. Centini, G. Leahu, F. Mura, S. Sennato, C. Sibilia, V. Robbiano, M. C. Giordano, C. Martella, D. Comoretto, and F. Buatier de Mongeot, Advanced Optical Materials 2, 208–213 (2014).
19. A. Belardini, A. Benedetti, M. Centini, G. Leahu, F. Mura, S. Sennato, E. Fazio, C. Sibilia, V. Robbiano, M. C. Giordano, C. Martella, D. Comoretto, F. Buatier de Mongeot, Proc. SPIE 8772, 877203 (2013).
20. A. Benedetti, A. Belardini, A. Veroli, M. Centini, C. Sibilia, J. Appl. Phys. (2014) in press.
21. T. Verbiest , K. Clays , V. Rodriguez , Second-Order Nonlinear Optical Characterization Techniques , CRC Press , New York (2009).
22. A. Belardini, M. C. Larciprete, M. Centini , E. Fazio , C. Sibilia, D. Chiappe , C. Martella , A. Toma , M. Giordano , F. Buatier de Mongeot, Phys. Rev. Lett. 107 , 257401 (2011).
23. A. Belardini, E. Fazio, M. Centini, C. Sibilia, J. Haus, A. Sarangan, manuscript in preparation.